

AperTO - Archivio Istituzionale Open Access dell'Università di Torino

Encapsulation of Acyclovir in new carboxylated cyclodextrin-based nanosponges improves the agent's antiviral efficacy

This is the author's manuscript

Original Citation:

Availability:

This version is available <http://hdl.handle.net/2318/129648> since 2017-05-16T16:26:03Z

Published version:

DOI:10.1016/j.ijpharm.2012.12.031

Terms of use:

Open Access

Anyone can freely access the full text of works made available as "Open Access". Works made available under a Creative Commons license can be used according to the terms and conditions of said license. Use of all other works requires consent of the right holder (author or publisher) if not exempted from copyright protection by the applicable law.

(Article begins on next page)



UNIVERSITÀ DEGLI STUDI DI TORINO

This Accepted Author Manuscript (AAM) is copyrighted and published by Elsevier. It is posted here by agreement between Elsevier and the University of Turin. Changes resulting from the publishing process - such as editing, corrections, structural formatting, and other quality control mechanisms - may not be reflected in this version of the text. The definitive version of the text was subsequently published in

Int J Pharm;443(1-2):262-72. 2013 Feb 25. doi: 10.1016/j.ijpharm.2012.12.031.

<http://www.journals.elsevier.com/international-journal-of-pharmaceutics/>

You may download, copy and otherwise use the AAM for non-commercial purposes provided that your license is limited by the following restrictions:

- (1) You may use this AAM for non-commercial purposes only under the terms of the CC-BY-NC-ND license.
- (2) The integrity of the work and identification of the author, copyright owner, and publisher must be preserved in any copy.
- (3) You must attribute this AAM in the following format: Creative Commons BY-NC-ND license (<http://creativecommons.org/licenses/by-nc-nd/4.0/deed.en>), ***doi: 10.1016/j.ijpharm.2012.12.031.***

**Encapsulation of Acyclovir in new carboxylated cyclodextrin-based
nanosponges improves the agent's antiviral efficacy**

David Lembo¹, Shankar Swaminathan^{2,3§}, Manuela Donalisio¹, Andrea Civra¹, Linda Pastero⁴,
Dino Aquilano⁴, Pradeep Vavia³, Francesco Trotta⁵ Roberta Cavalli².

¹*Dipartimento di Scienze Cliniche e Biologiche, Università di Torino Ospedale S. Luigi Gonzaga, 10043
Orbassano, Torino, Italy*

²*Dipartimento di Scienza e Tecnologia del Farmaco, Università di Torino, via P. Giuria 9, 10125 Torino,
Italy*

³*Dep. of Pharmaceutical Sciences and Technology, University Institute of Chemical Technology, Mumbai,
400019, India*

⁴*Dipartimento di Mineralogia e Petrologia, Università di Torino, via V. Caluso 35, 10125 Torino, Italy*

[§]*Dipartimento di Chimica, Università di Torino, via P. Giuria 7, 10125 Torino, Italy*

[§]*Current adress: Hamilton Eye Institute, Department of Ophthalmology, University of Tennessee Health
Science Center, 930 Madison Avenue, Suite 731, Memphis, TN-38163, USA*

Corresponding author: Roberta Cavalli

Dipartimento di Scienza e Tecnologia del Farmaco

Via Pietro Giuria 9

Tel: 0039 116707825

Fax: 0039 11 6707687

roberta.cavalli@unito.it

Abstract

Cyclodextrin-based nanosponges (NS) are solid nanoparticles, obtained from the cross-linking of cyclodextrins, that have been proposed as delivery systems for many types of drugs. Various NS derivatives are currently under investigation in order that their properties might be tuned for different applications. In this work, new carboxylated cyclodextrin-based nanosponges (Carb-NS) carrying carboxylic groups within their structure were purposely designed as novel Acyclovir carriers. TEM measurements revealed their spherical shape and size of about 400 nm. The behaviour of Carb-NS, with respect to the incorporation and delivery of Acyclovir, was compared to that of NS, previously investigated as a drug carrier. DSC, XRPD and FTIR analyses were used to investigate the two NS formulations. The results confirm the incorporation of the drug into the NS structure and NS-Acyclovir interactions. The Acyclovir loading into Carb-NS was higher than that obtained using NS, reaching about 70 % w/w. *In vitro* release studies showed the release kinetics of Acyclovir from Carb-NS to be prolonged in comparison with those observed with NS, with no initial burst effect. The NS uptake into cells was evaluated using fluorescent Carb-NS and revealed the nanoparticle internalisation. Enhanced antiviral activity against a clinical isolate of HSV-1 was obtained using Acyclovir loaded in Carb-NS.

Key words: acyclovir, nanosponges, cyclodextrin, prolonged release, antiviral activity

1. INTRODUCTION

62

63 Acyclovir, a synthetic nucleoside analogue derived from guanosine, is a widely used antiviral
64 agent due to of its efficacy in the treatment of herpes simplex virus infections (O'Brien and
65 Campoli-Richards, 1989). However, neither the parenteral nor the oral administration of the
66 currently available formulations of Acyclovir is able to result in suitable concentrations of the
67 agent reaching at target sites. Acyclovir's absorption in the gastrointestinal tract is slow and
68 incomplete; of consequence, its pharmacokinetics following oral medication are highly variable
69 and its oral bioavailability ranges from just 10 to 30%. In general, around 80% of the
70 administered dose is not absorbed and current therapies therefore require the administration of
71 high doses, up to 1.2 g/day. As a consequence, the presence of systemic toxicity and adverse
72 reactions is frequent with its administration.

73 Many technological approaches, such as pro-drug preparations and innovative formulations, have
74 been proposed for improving the efficacy of Acyclovir treatment and decreasing its adverse side
75 effects. In recent years, the design of new delivery systems for the administration of antivirals
76 has attracted much research attention (Lembo and Cavalli, 2010). A number of Acyclovir
77 nanoparticulate systems have been developed, including nanoparticles (Giannavola et al., 2003;
78 Kamel et al., 2009; Yin et al., 2006; Cavalli et al., 2009; Bertino Ghera et al., 2009; Elshafeya et
79 al, 2010), liposomes (Pavelic et al., 2005; Chetoni et al. 2004), niosomes (Mukherjee et al., 2007;
80 Attia et al. 2007) and microemulsions (Gosh et al., 2006; Shishu et al. 2009), all of which aim at
81 improving the bioavailability of Acyclovir for either systemic or topical administration.

82 The present work focuses on the potential use of new β -cyclodextrin-based nanosponges (NS) as
83 specifically prepared novel Acyclovir carriers. Cyclodextrin-based NS are solid nanoparticles
84 consisting of highly cross-linked cyclodextrins, and were recently developed as a novel
85 nanoparticulate delivery system (Trotta and Cavalli, 2009; Trotta et al., 2012). This new
86 nanostructured material is prepared by reacting cyclodextrin (CD) with several cross-linking
87 agents: generally, activated carbonyl compounds (e.g. carbonyldiimidazole), pyromellitic
88 dianhydride and carboxylic acids. The reaction produces nanoparticles with a rather spherical
89 shape that possess the capacity to form stable nano-suspensions when dispersed in water under
90 stirring. NS show good biocompatibility and negligible biotoxicity. For example, the acute
91 systemic toxicity of nanosponges was evaluated in mice following the injection of doses that
92 varied between 500 mg and 5000 mg/Kg; the mice showed no signs of toxicity or any adverse

reactions. Their oral administration has also been tested in mice, with no apparent side effects noted (Trotta et al. 2012).

Nanosponges are highly efficient at entrapping different types of molecules (both organic and inorganic), and they can achieve this by means of inclusion or non inclusion complex formation. NS are able to complex with drug molecules due to their highly cross-linked structure and their many CD cavities, which can cooperate in forming inclusion complexes. Moreover, the polymer mesh forms a network with nano-channels able to entrap the guest molecules. This peculiar structural organisation favours molecule complexation and might be responsible for the increased solubility, stabilisation and protection capacities of nanosponges in comparison with its parent cyclodextrins.

Cyclodextrin-NS have been exploited as carriers for various types of drugs, but in particular for molecules with poor aqueous solubility (Cavalli et al., 2006; Swaminathan et al., 2007 and 2010; Ansari et al., 2010; Mognetti et al. 2012). Recently, loading NS with paclitaxel was found to increase the bioavailability of the drug when orally administered to rats compared to that obtained for free paclitaxel (Torne et al., 2010). Further studies demonstrated the ability of NS to increase the solubility and the oral bioavailability of other molecules, including resveratrol and tamoxifen (Ansari et al., 2011; Torne et al., 2012). Based on these findings, the current work investigates the potential for cyclodextrin-NS to increase the oral bioavailability of Acyclovir.

The aim of this study was to develop new β -CD nanosponges purposely tuned for the formulation of Acyclovir, a drug with medium polarity and solubility. To this end, a new type of NS-derivative, containing dissociable carboxylic groups, was considered for the encapsulation of Acyclovir and its behaviour compared to the β -cyclodextrin-based NS that has previously been investigated in relation to more lipophilic drugs. The synthetic rationale consisted of increasing drug incorporation by increasing complexation due to electrostatic interactions between the acid groups belonging to the NS structure and the Acyclovir amino group. The physico-chemical characterisation of the Acyclovir NS formulations along with their *in vitro* antiviral activities are herein reported.

2. MATERIALS AND METHODS

2.1 Materials

Acyclovir, fluoresceine isothiocyanate, carbonyldiimidazole and ammonium acetate were purchased from Sigma-Aldrich (USA). Cyclodextrin was a kind gift from Roquette (Lestrem, France). All solvents used are of HPLC grade. All reagent used are of analytical grade. Milli Q water was used for all the experiments.

2.2 Synthesis of carbonate and carboxylate nanosponges

In this work, two different types of cyclodextrin-based NS, namely carbonate and carboxylate NS, were synthesised.

Carbonate NS were prepared as previously reported (Trotta and Cavalli, 2009; Trotta et al., 2012). Briefly, an amount of anhydrous cyclodextrin was dissolved in anhydrous DMF and allowed to react with carbonyldiimidazole at 90 °C for at least 5 h. Once the reaction was over, a large excess of water was added to destroy the excess of carbonyldiimidazole and the solid recovered by filtration. Then, the solid was ground in a mortar and Soxhlet-extracted with ethanol to remove residual reaction by-products. The reaction was carried out using a molar excess of crosslinker (e.g. 1:4 of β CD:cross-linker). Following purification, NS were stored at 25 °C.

New carboxylated nanosponges (Carb-NS) were obtained by reacting succinic anhydride on preformed NS in DMSO at 90 °C for 3 h. The solid nanosponges was recovered by filtration and washed with a large amount of water. The presence of carboxylic groups in the structure was assessed by titrimetry with NaOH solution and by FTIR analysis (Perkin Elmer System 2000).

For titrimetry determination, a known amount of Carb-NS was dissolved in a KCl solution. After standing for a long time (i.e. 24 h) the suspension was titred with NaOH 0.1 M.

NS surface charge modification, determining the Zeta potential value, was also used to ascertain the presence of the acidic groups.

Finally, fluorescent Carb-NS were also synthesised for cellular trafficking studies. For this purpose, pre-formed NS were added to a fluorescein isothiocyanate solution in DMSO and incubated at 90 °C for 3 h. Then, the solid was recovered by filtration and washed with ethanol. The dried product was reacted with the succinic anhydride as previously described to obtain fluorescent Carb-NS.

2.3 Preparation of Acyclovir-loaded nanosponges

A weighed amount of Acyclovir was dispersed in aqueous suspensions (pH=5.5) of both NS and carb-NS in a weight ratio of 1:4 and magnetically stirred for 24 h. Suspensions were then centrifuged at 2000 rpm for 10 min to separate out the non-complexed drug as a residue below the colloidal supernatant. The colloidal supernatants were freeze-dried using a Modulyo freeze-drier (Edwards, UK) to obtain the drug-loaded nanosponges. The two drug-loaded NS formulations were stored in a covered vacuum desiccator at ambient temperature until further use. Nanosponge nanosuspensions were sterilised by autoclaving (121°C, 2 bar) for the biological studies.

2.4 Physical mixture preparation

Binary physical mixtures were prepared by mixing Acyclovir and the two dried NS types in a glass mortar (4:1 nanosponge:Acyclovir weight ratio).

2.5 Acyclovir quantitative determination

The quantitative determination of Acyclovir was achieved by HPLC analysis using a Perkin Elmer instrument (L2 Binary Pump, Perkin Elmer) with a UV-vis spectrophotometer detector (LC 95, Perkin Elmer, USA) with an external standard method. A reverse-phase hypersil ODS column (25 cm x 4.6 mm Varian, USA) was used with a mobile phase consisting of a 12:88 (v/v) ratio of acetonitrile:20 mM ammonium acetate buffer pH=3.5 and a flow rate of 1 ml/min. The UV detector wavelength was set to 250 nm. The calibration curve is linear in the range 0.5-15 µg/ml with a r^2 of 0.9997. For cellular studies, the HPLC method for Acyclovir determination was tuned by changing the mobile phase to a ratio of water (adjusted to pH 2.5 with orthophosphoric acid):methanol (92:8); the same flow rate of 1ml/min was used and UV detection was carried out at 252 nm.

2.6 Determination of size, polydispersity index and zeta potential of nanosponges

NS sizes and polydispersity indices were measured by dynamic light scattering using a 90 Plus particle sizer (Brookhaven Instruments Corporation, USA) equipped with MAS OPTION particle sizing software. The measurements were made at a fixed scattering angle of 90° and 25°C for all samples. The samples were suitably diluted with filtered distilled water before every measurement. Zeta potential measurements were also made using an additional electrode in the same instrument. For zeta potential determination, all NS formulations were diluted with 0.1 mM KCl and placed in the electrophoretic cell, where an electric field of about 15 V/cm was applied.

2.7 Morphology evaluation of nanosponges

Transmission electron microscopy (TEM) was employed to evaluate the shape of the NS formulations. A Philips CM 10 transmission electron microscope was used, and particle size was measured using NIH image software. NS suspensions, at a concentration of 0.5 % w/v of NS, and Carb-NS (either loaded or unloaded) were sprayed on Formwar-coated copper grids and air-dried before observation.

2.8 Determination of Acyclovir loading

A weighed amount (5 mg) of both Acyclovir-loaded NS and Carb-NS was dispersed into water, sonicated for 30 min and then diluted in a mixture of water (adjusted to pH 2.5 with orthophosphoric acid): methanol (92:8, v/v). After centrifugation the supernatant was analysed by HPLC after suitable dilution, as described before.

2.9 *In vitro* release of Acyclovir from nanosponges

The *in vitro* release studies were carried out using multi-compartment rotating cells with a dialysis membrane (Sartorius, cut off 12,000 Da). The donor phase consisted of NS suspension containing a fixed amount of Acyclovir in phosphate buffer at pH 7.4 (1 ml). The receiving phase, which consisted of phosphate buffer pH 7.4, was completely withdrawn and replaced with

fresh medium after fixed time intervals, suitably diluted and analysed using the above described HPLC method. The experiment was carried out in triplicate.

2.10 Differential Scanning Calorimetry

Differential Scanning Calorimetry (DSC) was carried out using a Perkin Elmer DSC/7 (Perkin-Elmer, CT, USA) equipped with a TAC 7/DX instrument controller. The instrument was calibrated with indium for melting point and heat of fusion. A heating rate of 10°C/min was employed in the 25–300°C temperature range. Standard aluminium sample pans (Perkin-Elmer) were used; an empty pan was used as reference standard. Analyses were performed in triplicate on 5 mg samples under nitrogen purge at a flow.

2.11 X-Ray Powder Diffraction (XRPD)

Plain Acyclovir, Acyclovir physical mixtures, Acyclovir-loaded NS and Acyclovir-loaded Carb-NS loaded were examined by XRPD. Diffraction data were collected using a Panalytical X'Pert Pro diffractometer (Bragg Brentano geometry, Cu $K\alpha_{1,2}$ radiation) and a Huber Guinier Camera G670 (Cu $K\alpha_{1,2}$ radiation). Diffraction profiles were analysed using the curve fitting and analysis FITYK software (Wojdyr, 2010). A Pearson VII shape profile was used for the diffraction pattern decomposition in order to simulate better the sample and instrumental contributions to the diffraction. The peak profile we selected takes account of the effect of the presence of a $K\alpha_{1,2}$ radiation.

2.12 Fourier Transformed Infra-Red (FT-IR) Spectroscopy

Fourier Transform spectroscopy (FTIR) was carried out on Acyclovir loaded NS, Acyclovir-loaded Carb-NS and plain drug using a Perkin Elmer system 2000 spectrophotometer to understand whether structural differences exist between the different NS systems. The spectra were recorded within the interval 4000 to 650 cm^{-1} using KBr pellets.

2.13 Biological studies

Cells and Viruses

African green monkey fibroblastoid kidney cells (Vero) were grown as monolayers in DMEM supplemented with 10% heat-inactivated foetal calf serum and antibiotics. A clinical isolate of HSV-1 (HSV-1 MRC) sensitive to Acyclovir was provided by Dr. Piro, Amedeo di Savoia Hospital, Turin, Italy.

Cell viability assay

To test the cytotoxic effect of Acyclovir, Acyclovir-loaded NS and Acyclovir-loaded Carb-NS, Vero cells were seeded at a density of 6×10^4 /well in 24-well plates. After 24 h, they were either incubated with the compounds or left untreated. After 72 h treatment, cell viability was determined by the 3-(4,5-dimethylthiazol-2-yl)-2,5-diphenyltetrazolium bromide (MTT) method, as previously described (Paules et al., 1988). The effect on cell viability of each formulation at different concentrations was expressed as a percentage by comparing treated cells with cells incubated with culture medium only.

Virus yield reduction assay

The effect of Acyclovir and the two formulations of Acyclovir-loaded NS on the production of infectious virus was assessed in yield reduction assays, where the cells were infected with virus at a multiplicity of infection (MOI) of 0.01 pfu/cell and then exposed to the drug for 72 h. After 1 h adsorption, the virus inoculum was removed and cultures were exposed in duplicate to serial dilutions of the test compound. Supernatants were pooled as appropriate 72 h after infection and cell-free virus infectivity titres were determined in duplicate by plaque assay in Vero cell monolayers. The end-points of the assay were the inhibitory concentrations of drug which reduced virus yield by 50% (IC_{50}) in comparison to the untreated virus control. The IC_{50} values were calculated for inhibition curves using the program PRISM 4 (GraphPad Software, San Diego, California, U.S.A.) fitted to a variable slope-sigmoidal dose-response curve.

Evaluation of cellular uptake by confocal laser scanning microscopy

Exponentially growing Vero cells were plated and cultured overnight in 24-well plates on glass coverslips. Subsequently, the cell monolayers were incubated with 10 μ M of the labelled compounds for the indicated time points and then extensively washed with PBS for the

observation of the living cells. Confocal sections were taken on an inverted Zeiss LSM510 fluorescence microscope.

Determination of Acyclovir concentration in Vero cells

The concentration of Acyclovir in Vero cells was investigated as a measure of the intracellular accumulation of the drug. After incubation with plain Acyclovir or the Acyclovir formulations, the cells were washed, lysed with a saturated solution of ammonium sulphate and then centrifuged at 4 °C for min. Cell lysates were frozen and stored at -18°C. Immediately prior to their analysis, cell lysates were thawed and centrifuged at 5000 rpm for 10 min at 10°C. The supernatants were diluted with the mobile phase, vortexed for 5 min and injected into the HPLC system, as described above in relation to the estimation of the Acyclovir concentration. The amount of Acyclovir taken up inside the cells was calculated from the standard curve obtained in the mobile phase with blank cellular lysate added to varying amounts of drug stock solution. Enhanced cell uptake of Acyclovir-loaded NS and Carb-NS was expressed as a % of the uptake of plain Acyclovir.

2.14 Statistical analysis

The results are expressed as mean \pm SD. Statistical analyses were performed using unpaired Student's t-test. A value of $p < 0.05$ was considered significant.

3. RESULTS AND DISCUSSION

Acyclovir is an antiviral molecule of medium polarity and a solubility of 1.5 mg/ml. It is reported in the BCS classification developed by Gordon Amidon (Amidon et al., 1995) as a class III drug; i.e. soluble with low intestinal permeability. The development of formulations for drugs belonging to this class can be challenging and the solubility/dose ratio can be a key parameter. As a consequence, Acyclovir needs to be administered in large doses, either orally or intravenously, to obtain the therapeutic effect desired. The solubility of the drug can play a

critical role. Indeed, Acyclovir is available on the market as a solution for parenteral administration, but the precipitation of the drug can easily occur when its solubility is exceeded; consequently, renal tubular damage may occur following intravenous administration. Thus, new formulations of Acyclovir using innovative approaches aim at decreasing the daily doses and, in turn, the adverse side effects of the drug. One strategy would be to consider the application of nanocarriers for its deliver and, through their use, overcome some of the limitations of the drug associated with its conventional dosage forms (Lembo and Cavalli, 2010). Of the various compounds that have been investigated as potential carriers and solubilising agents, the use of cyclodextrin derivatives and cyclodextrin polymers has been proposed for a number of drugs (Martin del Valle, 2004; Van de Manakker et al, 2009; Loftsson and Brewster, 2010). Previous studies have shown that cyclodextrin cavities of sulphated amphiphilic derivatives are able to encapsulate Acyclovir, forming stable compounds (Dubes et al., 2003). Furthermore, a soluble β -CD/poly(amidoamine) copolymer carrying cyclodextrin cavities and a macromolecule chain was found to significantly increase the solubility of Acyclovir due to its high drug complexing capacity (Bencini et al., 2008).

In the present study, novel Carb-NS were purposely synthesised for Acyclovir formulation. Carboxylic groups were linked to the structure of preformed NS to enhance the interactions of the nanocarrier with Acyclovir, with the aim of increasing drug loading and stability. The marked change in the Carb-NS surface charge in comparison with that of NS provided evidence of the binding of carboxylic groups, but their presence in the nanosponge structure was firmly established by titrimetry experiments and FTIR analysis. Titrimetric analysis was able to determine a carboxylic group concentration of 1.1 mmol/ g of nanosponges.

The FTIR spectrum of Carb-NS differed markedly from that of NS (Fig.1): in particular, it shows a higher and broader peak in the region of the carbonyl group at about 1770 cm^{-1} and an increase in C=O stretching due to the addition of carboxylic groups.

Fig. 1

Carb-NS, when dispersed in water, formed nanosuspensions with ease and without the addition of stabiliser agents or surfactants. The average diameters, polydispersity indices and zeta

potentials of nanosponges are reported in Table 1. Considering the particle sizes, no important differences are detectable between loaded and unloaded nanosponges.

Both types of NS have an average diameter of approx. 400 nm, rather narrow size distributions, and polydispersity indices ranging between 0.11 and 0.13.

In contrast, the zeta potential values of the two NS types are very different. The surface charge of Carb-NS (-38.3 mV) is more negative than that of NS (-25.4 mV), confirming the presence of the carboxylic groups in its structure, but its zeta potential value is sufficiently high enough to ensure physical stability between nanosponge particles through electrostatic repulsion, and thereby avoiding aggregations. The NS dispersed in water were confirmed to be stable for six months when stored at 4 °C and presented no precipitation phenomena. The sterilisation process did not affect nanosponge sizes, as previously shown (Swaminathan et al., 2010).

Fluorescent Carb-NS did not show larger sizes or higher polydispersity index values than those of Carb-NS (Table 1).

Table 1

To investigate NS size and morphology further, microscopy studies were carried out using TEM analysis. TEM photomicrographs of the two types of loaded nanosponges are reported in Fig. 2 and confirm their previously ascertained sizes. Acyclovir-loaded nanosponges were spherical in shape with a rather uniform distribution.

Fig. 2

Both types of nanosponges were able to incorporate Acyclovir. The presence of the carboxylic groups in the Carb-NS structure markedly affected drug loading compared to that of unmodified NS; the drug loading percentages for NS and Carb-NS were 38 % and 69 % w/w, respectively. This strong difference could be ascribed to the presence of the acid groups in the Carb-NS structure acting as further sites for Acyclovir electrostatic interactions besides the cyclodextrin cavities.

The Acyclovir interaction with both NS types was confirmed by DSC, XRPD and FTIR analyses. The DSC thermograms of the two types of Acyclovir-loaded NS are showed in Fig. 3.

Fig. 3 DSC

As reported in Figure 3, Acyclovir shows an endothermic peak at approx. 260°C ($T^{\text{peak}} = 266.7$) corresponding to Acyclovir fusion, which is absent following its inclusion into nanosponges (either Carb-NS or NS). The disappearance of the drug peak in the DSC thermograms may indicate that Acyclovir is unable to crystallise and that it is mainly molecularly dispersed in the nanosponge structure. This behaviour confirms Acyclovir's interaction with the nanosponge structure. Conversely, the Acyclovir peak is clearly detectable in the drug physical mixture.

The mode of interaction between Acyclovir and the two nanosponges was then evaluated by XRPD analysis. From XRPD analysis, we can qualitatively obtain an estimate of the crystallinity grade of the sample. Sharp peaks with high *Intensity* versus *Half Width at Half-Maximum* ratios (I/hw_{hm}) are typically due to well-crystallised compounds (the spread of the interplanar spacing around the median value is small). On the contrary, large peaks (low I/hw_{hm} values) are representative of poorly crystalline materials with a large spread of the d_{hkl} around the median value. Plain Acyclovir is a well-crystallised drug and shows a complex diffraction pattern with sharp and defined diffraction peaks (Fig.4).

Fig. 4

Fig. 5 and Fig 6 report XRPD patterns of drug-loaded NS formulations compared to the XRPD pattern of plain NS. The crystallinity of Acyclovir decreased following its loading into NS, proving that drug interaction complexation is not due to a mechanical mixing of the components. These data lie in agreement with the DSC results.

Fig 5 and Fig. 6

Fig. 7 reports the decomposition of the experimental XRPD diffraction profiles of plain NS and plain Carb-NS. From Fig.7 it comes out that the diffraction peaks of NS are very large. This means that we are dealing not with a crystalline phase but with substances that tend to the amorphisation. As a matter of fact, the shape obtained from the peak profile decomposition procedure is essentially Gaussian, confirming their low degree of crystallinity, as expected when dealing with “amorphous-like” materials. As previously reported, NS can be obtained, either in crystalline form or in paracrystalline phase (amorphous state), from a β -CD cross-linking reaction modifying the synthetic procedure (Swaminathan et al., 2010).

Fig. 7

Table 2, which is related to Fig.7, reports the peak position values (2θ) and the corresponding interplanar spacing (d_{hk}) of plain NS and Carb-NS. The structural partial and weak ordering is quite different between NS and Carb-NS, resulting in longer-range ordering in the non-carboxylated NS. The addition of carboxylic groups on the structure was confirmed by the displacement of peak positions.

Table 2

The analyses of physical mixtures of both types of NS with Acyclovir evidenced no interaction between the drug and carrier. In Fig. 8, the decomposition analysis of the diffraction peaks of the Carb-NS physical mixture is reported. As expected, the physical mixture of Carb-NS and drug shows the individual diffraction patterns superimposed. The 2θ position of the reflections of the two phases is unaltered, as expected from a physical mixture which is free from chemical interaction.

Fig. 8

FTIR studies showed the presence of interactions between Acyclovir and Carb-NS or NS that were evident from peak broadenings and peak disappearance in the Acyclovir-loaded samples as illustrated in Figure 9. The prominent characteristic peaks of Acyclovir were found at around 1200 to 1600 cm^{-1} . All the characteristic peaks of Acyclovir in that range were modified in the formulations of the drug with the two types of nanosponges, suggesting definite interactions between drug and nanocarrier.

Fig. 9

The *in vitro* release profiles of Acyclovir from the two types of nanosponges are reported in Figure 10.

Fig 10

A sustained release of the drug from the two types of NS was observed indicating the encapsulation of Acyclovir within the nanostructures. The percentages of Acyclovir released from Carb-NS and NS after 3 h *in vitro* were approx. 22% and 70%, respectively. No initial burst effect was observed for either formulation, proving that the drug was not weakly adsorbed onto the nanosponge surfaces. These results lie in agreement with those obtained from Acyclovir incorporation in other nano-delivery systems (Cavalli et al, 2009; Bertino Ghera et al., 2009) where a prolonged release of Acyclovir was observed. The slower release kinetics obtained for Acyclovir loaded in the Carb-NS formulation might be related to a stronger complexation due to the additional electrostatic interaction of the carboxylic groups with the Acyclovir amino groups.

Plain Acyclovir was found to dissolve rapidly, and an equilibrium between the two compartments of the *in vitro* release system was reached in just a few minutes (data not shown).

Neither Acyclovir, nor NS nor Carb-NS exhibited significant cytotoxic effects on Vero cells as indicated in Figure 11.

Fig. 11

To compare the antiviral activities of plain Acyclovir, Acyclovir-loaded NS and Acyclovir-loaded Carb-NS, a virus yield reduction assay was performed using monolayers of Vero cells infected with a clinical isolate of HSV-1. This isolate is sensitive to the inhibitory activity of Acyclovir (Bencini et al., 2008) and the assay provides a stringent test allowing multiple cycles of viral replication to occur before measuring the production of infectious viruses. The dose-response curve shown in Figure 12 demonstrates that the antiviral potency of the Acyclovir-loaded Carb-NS was higher than that of free Acyclovir. By contrast, the Acyclovir-NS complex displayed an antiviral activity similar to that of free Acyclovir. The different behaviours observed between the two types of NS might be ascribed to the high drug loading and the slower kinetics of release obtained with Carb-NS.

The IC_{50} value for the Acyclovir-loaded Carb-NS determined at 72 h was found to be 0.033 μ M (95%CI: 0.025-0.043 μ M) while those obtained for Acyclovir-NS and free Acyclovir were 0.162 μ M (95% CI: 0.130-0.202 μ M) and 0.166 μ M (95% CI: 0.112-0.244 μ M), respectively. The IC_{50} value for plain Acyclovir corresponded to previously published values (Cavalli et al., 2009). The unloaded carriers exhibited no antiviral activity *per se* (data not shown).

Fig.12

We speculated that the difference in the antiviral activity between the two types of NS might be related to the different release kinetics of the drug. Acyclovir is more slowly released from Carb-NS than from NS, thus loaded nanosponges retaining a high Acyclovir payload might be internalised in cells.

This hypothesis could be proved by the evaluation of the cell uptake capacity of the NS formulations. The internalisation of nanoparticulate systems differed from that of the free molecules in solution (Cavalli et al., 2009). This was investigated by determining the accumulation of Acyclovir in the cells; the intracellular concentration of the drug was

considerably higher when the cells were incubated with Acyclovir-loaded Carb-NS compared with Acyclovir-NS or plain drug.

The percent enhancement of cellular uptake of Acyclovir formulations in Vero cells compared to that of the plain drug was approx. 70% for NS and more than 200% for Carb-NS.

On the strength of these results, in order to investigate whether acyclovir-loaded Carb-NS could deliver the drug inside cells, the cellular uptake of the formulation was evaluated by confocal laser scanning microscopy. For this purpose, fluorescent Carb-NS were used. The assay was carried out on living unfixed cells to avoid the occurrence of artefacts caused by cell fixation protocols.

Fig. 13

The results reveal a cytoplasmic distribution of fluorescent Carb-NS after 1 hour of its exposure to the cells, showing that the loaded NS are indeed internalised (Fig.13). No intracellular fluorescence was detected in control cells unexposed to the labelled compounds, (data not shown).

4. CONCLUSIONS

The ability of cyclodextrin to form inclusion complexes with various molecules is widely exploited in the pharmaceutical field to increase the solubility of lipophilic drugs. This technological approach for hydrophilic or medium polar drugs is less effective, thus the use of a cyclodextrin polymer presents a potential strategy to improve this limitation. Nanosponges are biocompatible cross-linked cyclodextrin polymers, whose production is flexible and cost-effective thank to a simple synthesis and purification procedure along with the use of a limited number of reagents.. One noteworthy property of nanosponges is that they are able to encapsulate a variety of different types of molecule. In the present study, new Carb-NS were purposely prepared as the carrier for Acyclovir and evaluated *in vitro* in comparison with previously studied nanosponges. Carb-NS were spherical in shape with a mean diameter of

approximately 400 nm; they possessed a rather narrow polydispersity index and sufficiently high negative surface charges to form stable nanosuspensions in water.

Carb-NS showed enhanced drug loading and more prolonged release kinetics in comparison with NS. Moreover, enhanced *in vitro* antiviral efficacy was observed when Acyclovir was encapsulated within Carb-NS. Considering the biocompatibility of nanosponges, the development of Acyclovir-loaded nanosponge formulations holds great potential for their use in various administration routes. In conclusion, this supramolecular technology should be considered as a promising platform that could be extended to other antiviral drugs with the aim of improving both drug formulation and antiviral activity

Acknowledgments

The research was supported by Turin University research funds

References

Amidon G.L., Lennernas H., Shah V.P., Cristin J.R., 1995. A theoretical basis for a biopharmaceutic drug classification-. the correlation of in vitro drug dissolution and in vivo bioavailability. Pharm. Res. 12, 413-420

Ansari K.A., Torne S. I, Vavia P.R., Trotta F., Cavalli R., 2010. Paclitaxel loaded nanosponges: in vivo characterization and cytotoxicity study on MCF-7 cell line culture. Curr. Drug Deliv. 8, 192-202

Ansari K.A., Vavia P.R., Trotta F., Cavalli R., 2011.Cyclodextrin-Based Nanosponges for Delivery of Resveratrol: In Vitro Characterisation, Stability, Cytotoxicity and Permeation Study. AAPS PharmSciTech.. 11, 279-286

Attia A., El-Gizawy A., Fouda A., 2007. Influence of a niosomal formulation on the oral bioavailability of acyclovir in rabbits, *AAPS PharmSciTech.* 8, E1-E4

Bencini M., Ranucci E., Ferruti P., Trotta F., Donalisio M., Cornaglia M., Lembo D., Cavalli R., 2008. Preparation and in vitro evaluation of the antiviral activity of the Acyclovir complex of a beta-cyclodextrin/poly(amidoamine) copolymer, *J. Control. Release.* 126 17–25.

Bertino Ghera B., Perret F., Chevalier Y., Parrot-Lopez H., 2009. Novel nanoparticles made from amphiphilic perfluoroalkyl α -cyclodextrin derivatives: Preparation, characterization and application to the transport of acyclovir. *Int. J. Pharm.* 375, 155-162

Cavalli R., Donalisio M., Cibra A., Ferruti P., Ranucci E., Trotta F., Lembo D., 2009. Enhanced antiviral activity of Acyclovir loaded into β -cyclodextrin-poly(4-acryloylmorpholine) conjugate nanoparticles. *J. Control Release.* 137, 116-122

Cavalli R., Trotta F., Tumiatti W., 2006. Cyclodextrin-based nanosponges for drug delivery. *J. Incl. Phenom. Macrocycl. Chem.* 56, 209-213

Chetoni P., Rossi S., Burgalassi S., 2004. Comparison of liposome encapsulated acyclovir with acyclovir ointment: ocular pharmacokinetics in rabbits. *J Ocul Pharmacol Ther.* 20, 169–77

Del Valle M. E. M., 2004. Cyclodextrins and their uses: a review. *Process Biochem.* 39, 1033-1046

Dubes A., Degobert G., Fessi H., Parrot-Lopez H., 2003. Synthesis and characterisation of sulfated amphiphilic α -, β - and γ cyclodextrins: application to the complexation of acyclovir. *Carbohydrate Res*, 338, 2185- 2193

Elshafeeya A. H., Kamel A. O., Awad G. A.S., 2010. Ammonium methacrylate units polymer content and their effect on acyclovir colloidal nanoparticles properties and bioavailability in human volunteers. *Colloids and Surf B: Biointerfaces.* 75, 398–404

565 Ghosh P. K., Majithiy R. J., Umrethia M.L., Murthy R. S. R., 2006. Design and Development of
 566 Microemulsion Drug Delivery System of Acyclovir for Improvement of Oral Bioavailability.
 567 AAPS PharmSciTech, 7, E1-E6
 568

569 Giannavola C., Bucolo C., Maltese A., Paolino D., Vandelli M.A., Puglisi G., Lee V. H. L.,
 570 Fresta M., 2003. Influence of Preparation Conditions on Acyclovir-Loaded Poly-*d,l*-Lactic Acid
 571 Nanospheres and Effect of PEG Coating on Ocular Drug Bioavailability. Pharm. Res. 20, 584-
 572 590
 573

574 Jin Y., Ping L. T., Li M., Houb X., 2006. Self-assembled drug delivery systems 1. Properties
 575 and in vitro/in vivo behavior of acyclovirself-assembled nanoparticles (SAN). International
 576 Journal of Pharmaceutics. 309, 199–207
 577

578 Kamel A., Awad G. A. S., Geneidi A. S., Mortada N. D., 2009. Preparation of Intravenous
 579 Stealthy Acyclovir Nanoparticles with Increased Mean Residence Time AAPS PharmSciTech.
 580 10,1427-1435
 581

582 Lembo D., Cavalli R., 2010. Nanoparticulate delivery systems for antiviral drugs, Antiviral
 583 Chemistry et Chemotherapy. 21, 53-70
 584

585 Loftsson T., Brewster M.E., 2010. Pharmaceutical applications of cyclodextrins: basic science
 586 and Product development. J. Pharm. Pharmacol. 62, 1119-1125
 587 Mognetti, B., Barberis, A., Marino S., Berta G., De Francia S., Trotta F., Cavalli R., 2012. In
 588 vitro enhancement of anticancer activity of paclitaxel by a Cremophor free cyclodextrin-based
 589 nanosponge formulation. J. Incl. Phenom. Macrocycl. Chem. .74, 201-210
 590

591 Mukherjee B., Patra B., Layek B., 2007. Sustained release of acyclovir from nano-liposomes and
 592 nano-niosomes: An in vitro study, Int. J. Nanomedicine. 2, 213–225
 593

594 O'Brien J.J., Campoli-Richards D.M., 1989. Acyclovir. An updated review of its antiviral
 595 activity, pharmacokinetic properties and therapeutic efficacy, Drugs. 37, 233–309.

596

597 Pauwels R., Balzarini J., Baba M., Snoeck R., Schols D., Hederwijn P., Desmyter J., De Clerq
 598 E., 1988. Rapid and automated tetrazolium-based colorimetric assay for the detection of anti HIV
 599 compounds. *J. Virol. Methods.* 20, 309–321.

600

601 Pavelic C., Skalko-Basnet N., Filipovic-Grcic J., 2005. Development and in vitro evaluation of a
 602 liposomal vaginal delivery system for acyclovir. *J. Controlled Rel.*, 106, 34– 43

603

604 Shishu, Rajan S., Kamalpreet, 2009. Development of Novel Microemulsion-Based Topical
 605 Formulations of Acyclovir for the Treatment of Cutaneous Herpetic Infections.
 606 *AAPS PharmSciTech.* 10, 560-565

607

608 Swaminathan S., Vavia P., Trotta F., Torne S., 2007. Formulation of cyclodextrin-based
 609 nanosponges of itraconazole. *J. Incl. Phenom. Macro. Chem.* 57, 89-94

610

611 Swaminathan S., Pastero L., Serpe L., Trotta F., Vavia P., Aquilano D., Trotta M., Zara G.P.,
 612 Cavalli R., 2010. Cyclodextrin-based nanosponges encapsulating camptothecin: physicochemical
 613 characterization, stability and cytotoxicity. *Eur. J. Pharm. Biopharm.* 74, 193-201

614

615 Torne S. J., Ansari K.A., Vavia P.R., Trotta F., Cavalli R., 2010. Enhanced oral paclitaxel
 616 bioavailability after administration of paclitaxel-loaded nanosponges. *Drug Delivery*, 17, 419-
 617 425

618

619 Torne S., Darandale S., Vavia P., Trotta F., Cavalli R., 2012. Cyclodextrin-based nanosponges:
 620 effective nanocarrier for Tamoxifen delivery. *Pharm Dev Technol.* Jan 12.

621

622 Trotta F., Cavalli R., 2009. Characterization and applications of new hyper-cross-linked
 623 cyclodextrins. *Composite Interfaces.* 16, 39-48

624

625 Trotta F., Zanetti M., Cavalli R., 2012. Cyclodextrin-based Nanosponges as drug carriers,
 626 *Belstein, J. Organic Chemistry* 8, 2091-2099

Van de Manakker F., Van Nostrum F., Hennik W.E., 2009. Cyclodextrin-Based Polymeric Materials: Synthesis, Properties and Pharmaceutical/Biomedical Applications Biomacromolecules. 10, 3157-3175

Wojdyr M., 2010. Fityk: a general purpose peak fitting program J. Appl. Cryst. 43, 1126- 1130

Figure captions

Figure 1 FTIR spectra of NS and Carb-NS.

Figure 2 TEM images of Acyclovir-loaded NS (left) and Acyclovir-loaded Carb-NS (right). (Magnification 46000x).

Figure 3 DSC thermograms (A and B) of the two types of Acyclovir loaded NS compared to plain NS, plain drug and physical mixtures.

Figure 4 Acyclovir XRD pattern. 2θ diffraction angle on the abscissa axis.

Figure 5 Comparison between XRPD patterns: plain NS (A), Acyclovir-loaded NS (B).

Figure 6 Comparison between XRPD patterns: plain Carb-NS (A), acyclovir-loaded Carb-NS (B).

Figure 7 XRPD decomposition for plain NS (A) and for plain Carb-NS (B).

Figure 8 (A) Decomposition of the diffraction pattern of a physical mixture of Carb-NS and Acyclovir (B) and (C) decompositions outline the contributions of the NS and drug, respectively.

Figure 9 FTIR spectra of acyclovir, acyclovir-loaded NS and acyclovir-loaded Carb-NS

650 Figure 10 Percentage of acyclovir released from NS and Carb-NS over time. Each point
651 represents the mean (n=3).

652 Figure 11 Effect of Acyclovir, NS and Carb-NS on the viability of non-infected Vero cells as a
653 function of the drug concentration at 72 h. X axis: nanosponge concentration, Y axis: cell
654 viability (% of untreated control). Each point represents the mean \pm S.D. (n=3).

655 Figure 12 Antiviral activity of free Acyclovir and Acyclovir loaded in NS or Carb-NS on a
656 clinical isolate of HSV-1. Vero cells were infected at a MOI of 0.01 and then exposed for 72 h to
657 different drug concentrations. Virus titres in the supernatants of cell cultures were determined by
658 standard plaque reduction assay. Values are the means of three separate determinations.

659 Figure 13 Cell uptake of fluorescent Carb-NS. Vero cells were incubated with the formulation
660 for the times indicated and then analysed by confocal laser scanning microscopy without
661 fixation. The upper panels show the fluorescence images while the lower panels show
662 fluorescence images merged with phase-contrast images.

663

663

664

Table captions

665

666

667 Table1: Particle sizes and zeta potentials of nanosponges

668

669 Table 2 Peak position occurrence between plain NS and plain Carb-NS

670

670

671

Table1: Particle sizes and zeta potential of nanosponges

Loaded Formulations	Average diameter \pm SD (nm)	Zeta Potential \pm SD MV	Polydispersity Index (PI)
NS	400 \pm 16	-25.4 \pm 2.7	0.12
Loaded-NS	403 \pm 19	-25.0 \pm 1.5	0.13
Carb-NS	410 \pm 12	-38.3 \pm 1.2	0.11.
Loaded Carb-NS	415 \pm 10	-28.2 \pm 1.7	0.12
Fluorescent Carb-NS	407 \pm 7	-35.3 \pm 1.2	0.12

672

673

673

674

Table 2 Peak position occurrence between plain NS and plain Carb-NS

	NS			Carb-NS		
2theta (°)	11.653	20.262	25.833	10.823	19.039	22.962
d _{hkl} (Å)	7.588	4.379	3.446	8.168	4.658	3.870

675

676

676

677

Figures of Acyclovir-Carb-NS paper

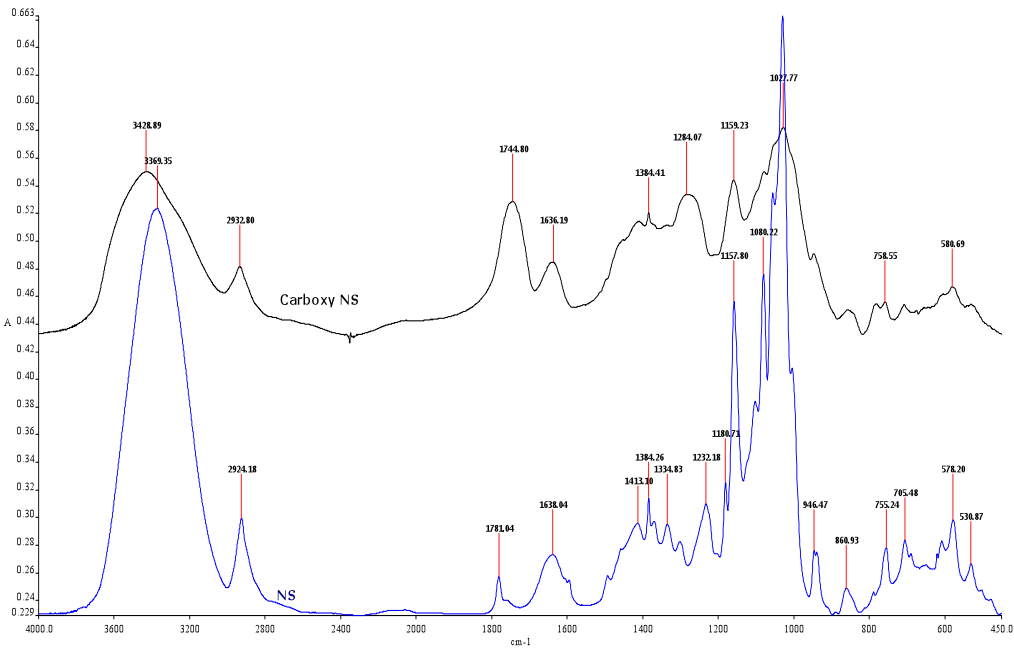


Fig.1

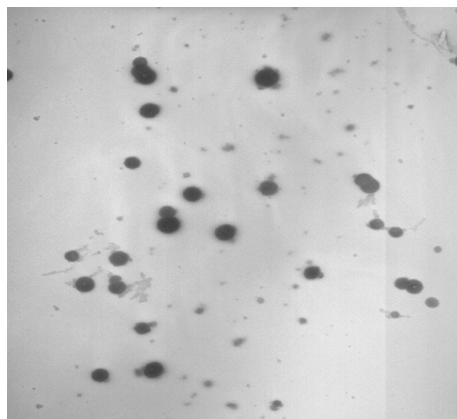
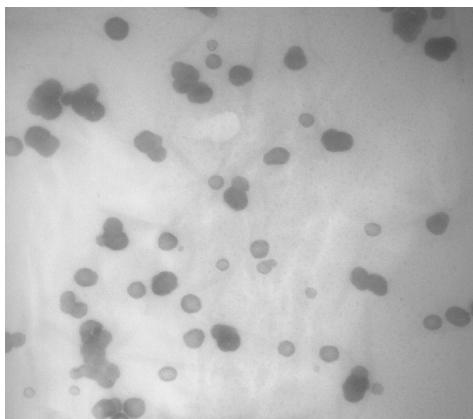


Fig. 2

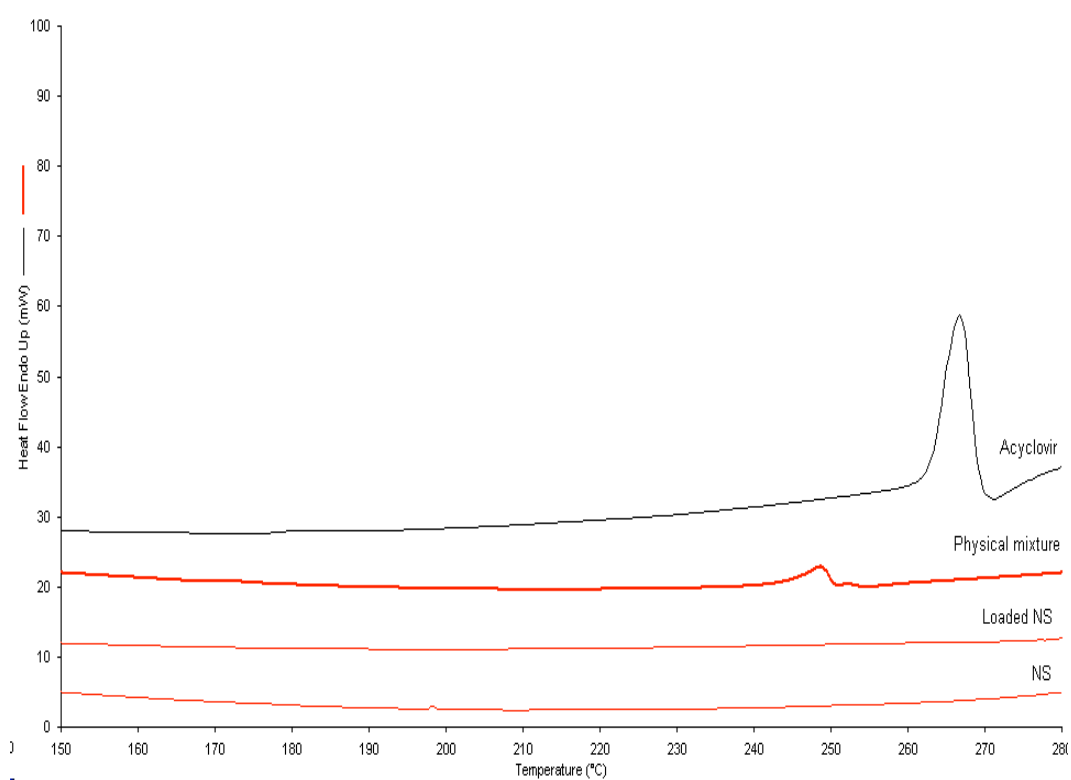


Fig. 3 (A)

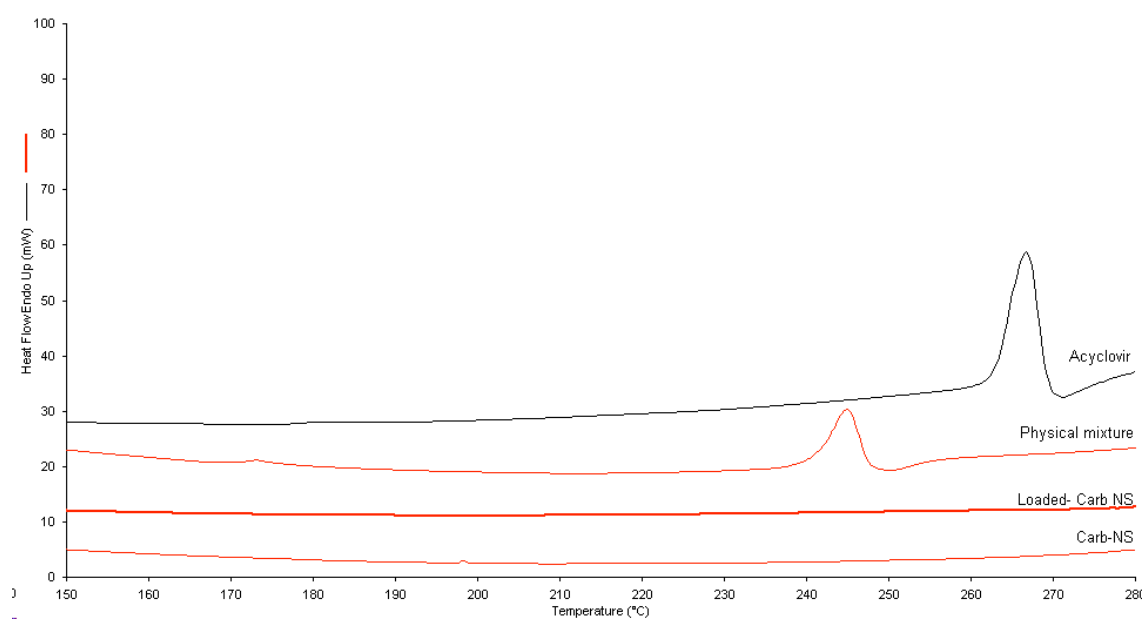


Fig. 3 (B)

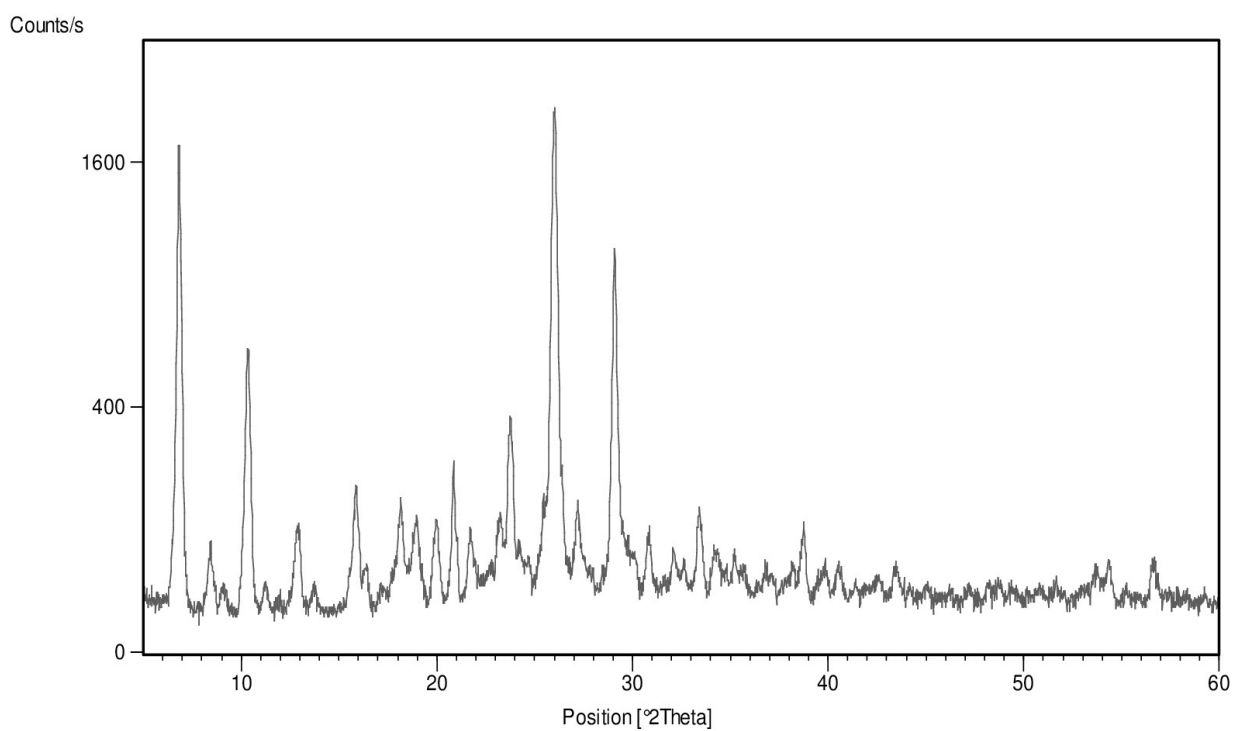


Fig. 4

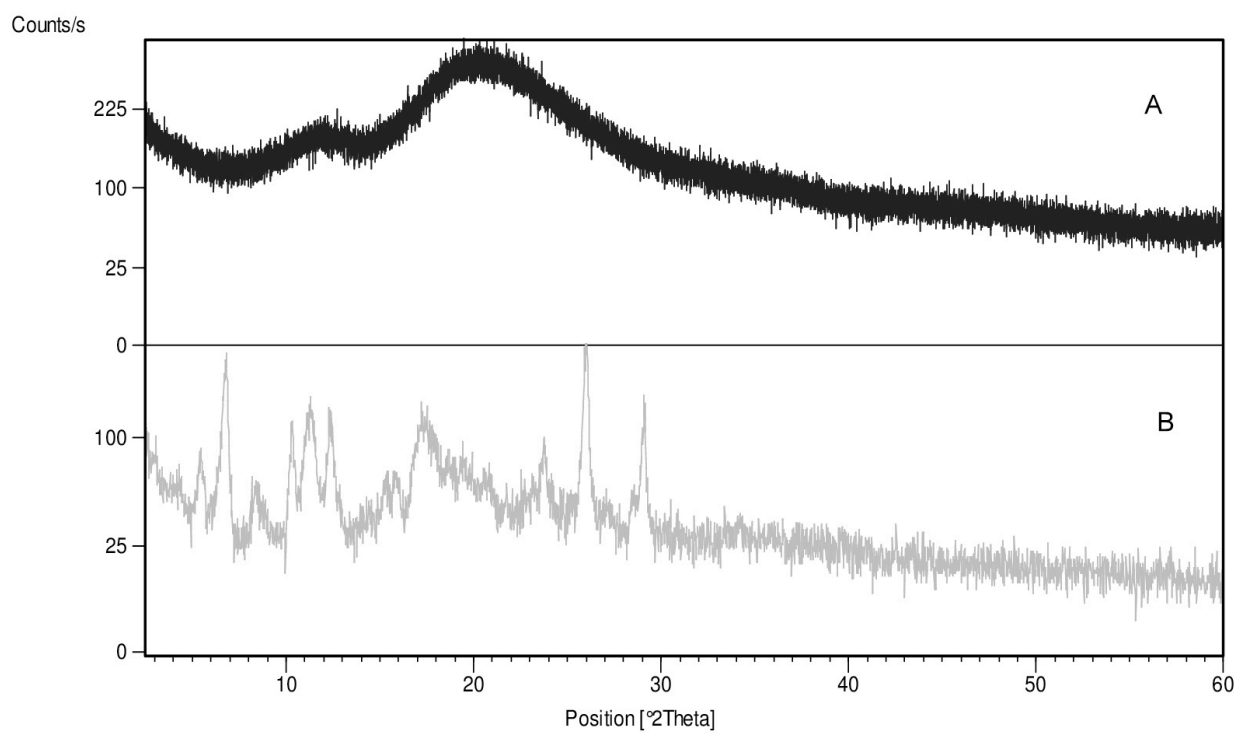


Fig 5

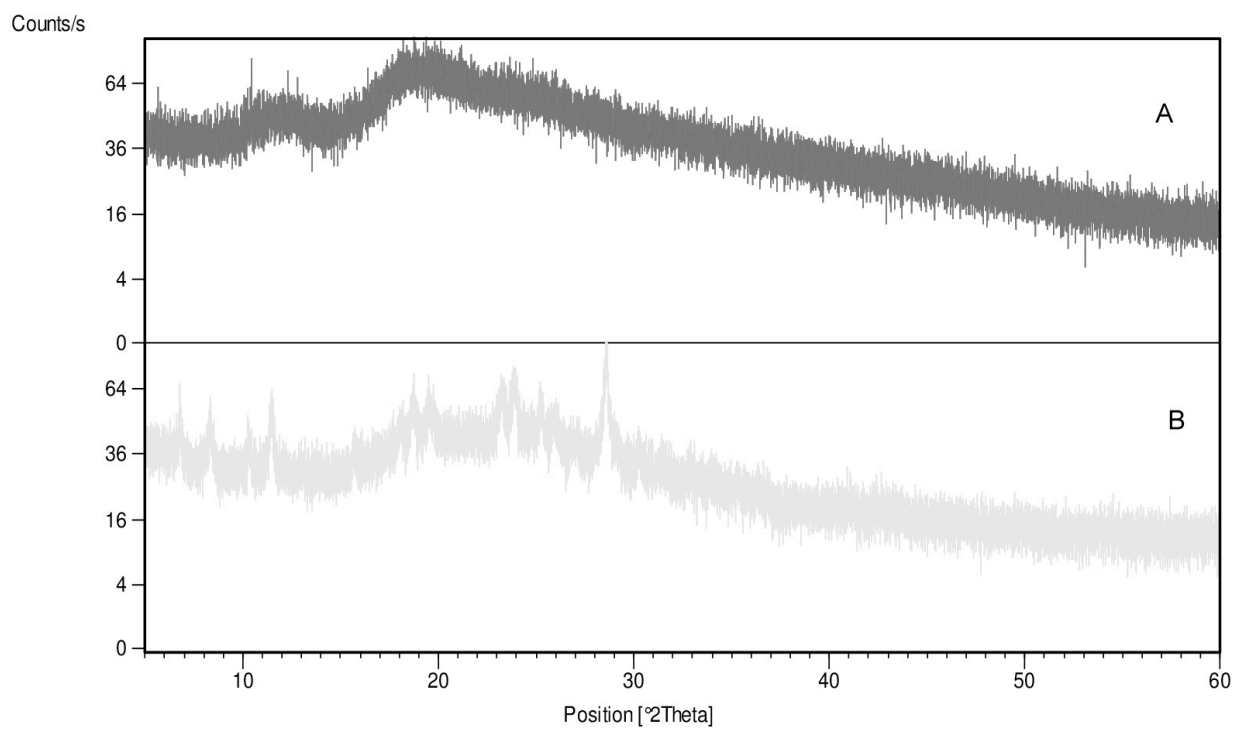


Fig.6

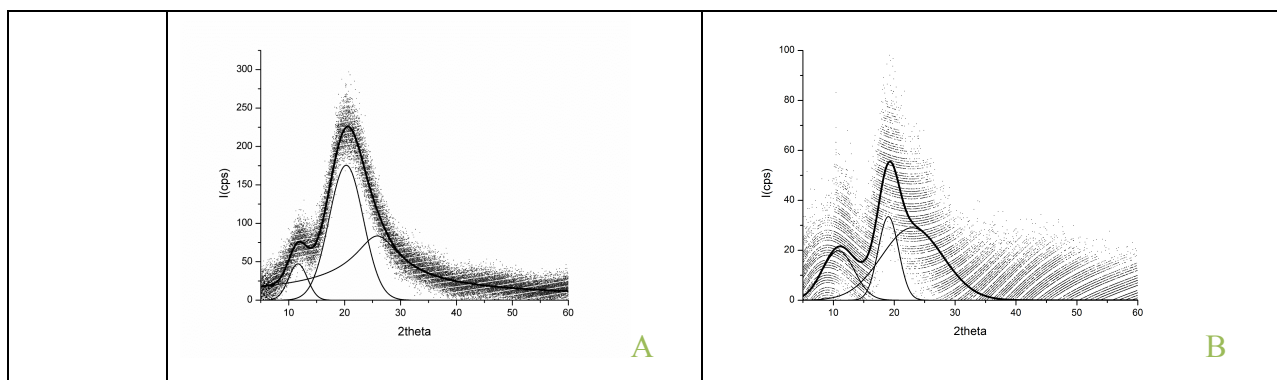


Fig 7

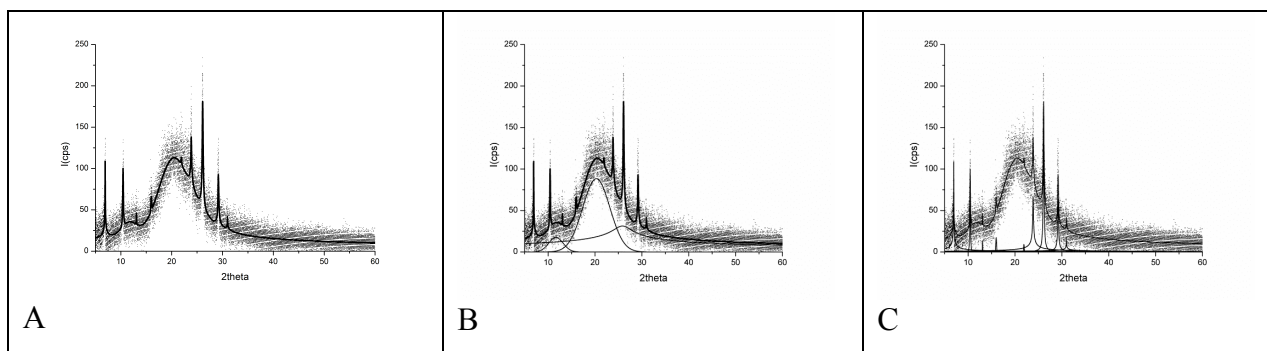


Fig.8

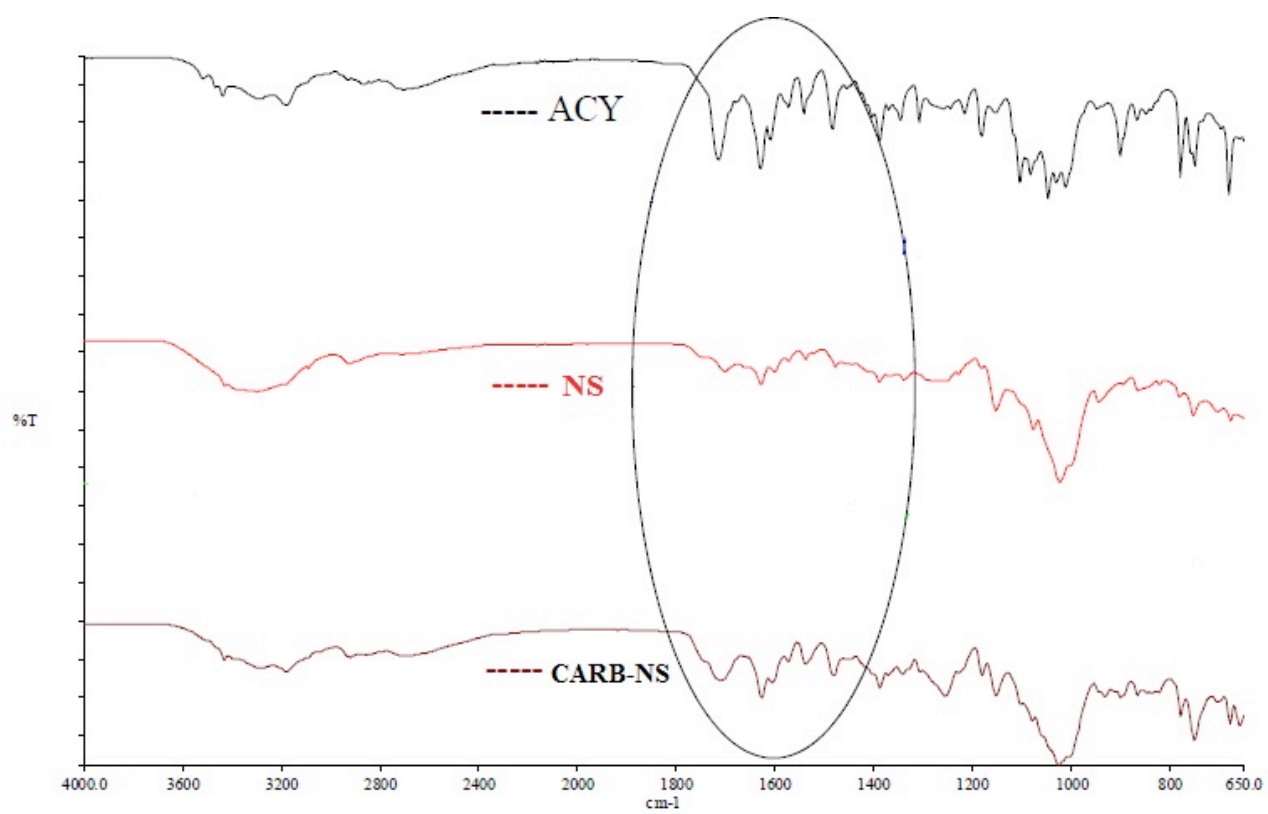


Fig. 9

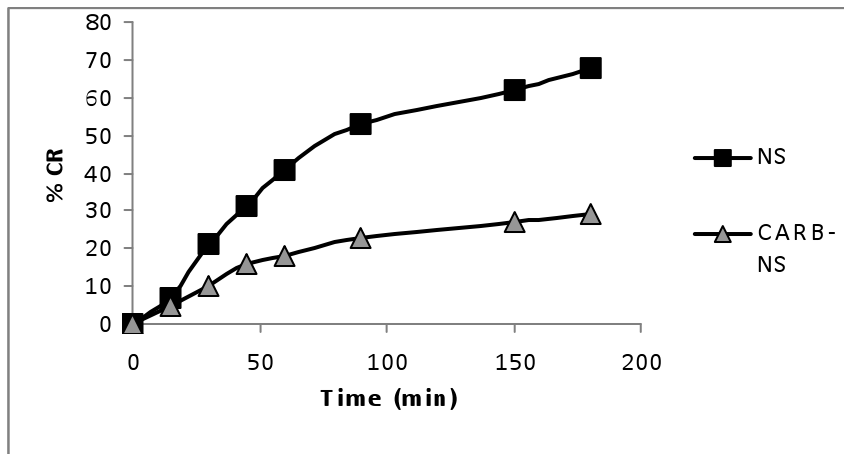


Fig.10

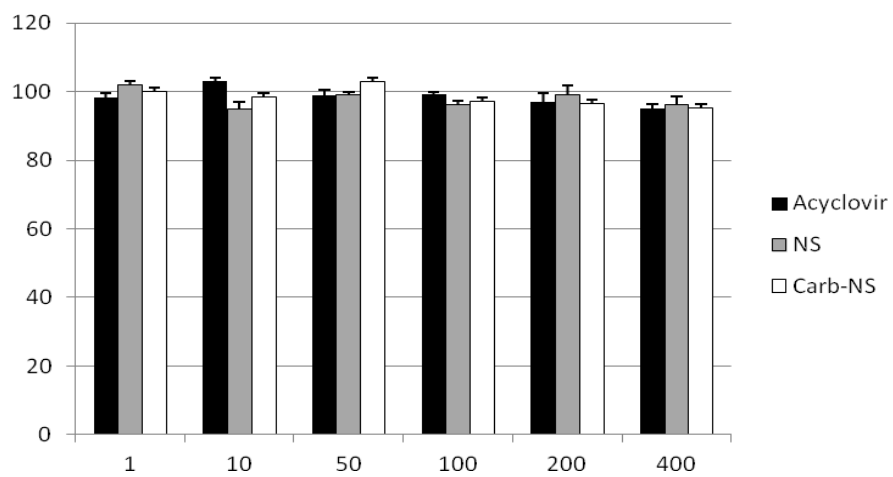


Fig 11

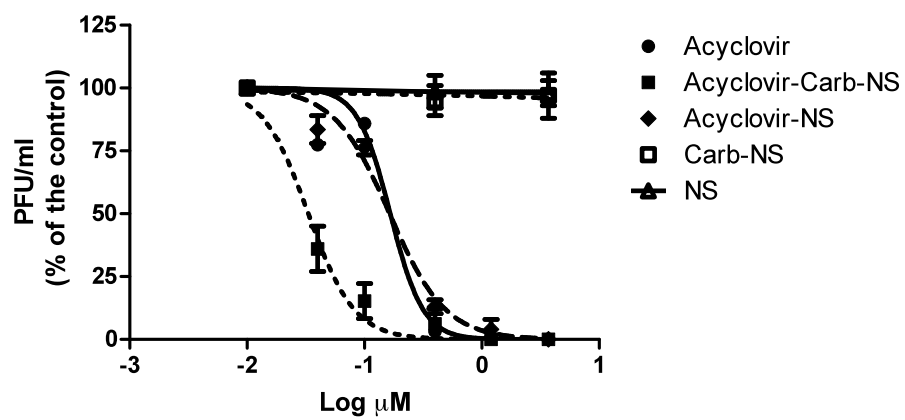


Fig. 12

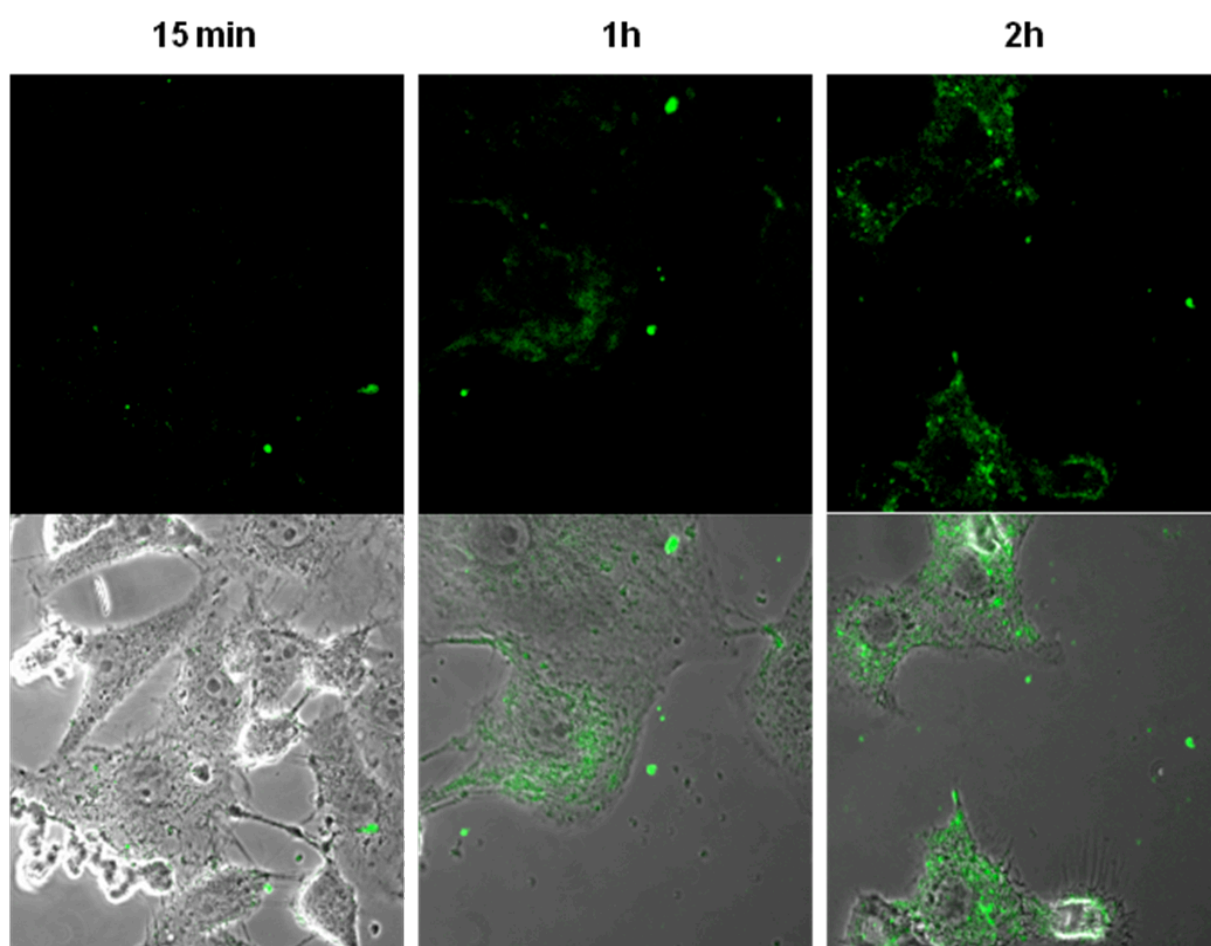


Fig. 13